applied sciences

MDPI

Article

Time-Domain Near-Infrared Spectroscopy in Subjects with Asymptomatic Cerebral Small Vessel Disease

Giacomo Giacalone [1,*], Marta Zanoletti [2], Rebecca Re [2,3], Davide Contini [2], Lorenzo Spinelli [3], Alessandro Torricelli [2,3] and Luisa Roveri [1]

[1] Neurology Department, San Raffaele Scientific Institute, Via Olgettina 48, 20132 Milan, Italy; roveri.luisa@hsr.it
[2] Dipartimento di Fisica, Politecnico di Milano, Piazza Leonardo da Vinci 32, 20133 Milan, Italy; marta.zanoletti@polimi.it (M.Z.); rebecca.re@polimi.it (R.R.); davide.contini@polimi.it (D.C.); alessandro.torricelli@polimi.it (A.T.)
[3] Istituto di Fotonica e Nanotecnologie, Consiglio Nazionale delle Ricerche, Piazza Leonardo da Vinci 32, 20133 Milan, Italy; lorenzo.spinelli@polimi.it
* Correspondence: giacalone.giacomo@hsr.it; Tel.: +39-(0)226432941

Abstract: Biomarkers of microcirculation dysfunction may help in the study of cerebral small vessel disease (CSVD). Time-Domain Near-Infrared spectroscopy (TD-NIRS), estimating the oxygenation of microcirculation of cerebral outer layers, might indirectly correlate with CSVD. We retrospectively evaluated TD-NIRS data from healthy subjects with age $\geq$ 55 years; no history of brain disease; normal neurological examination; absence of stenosis > 50% of extra/intra-cranial arteries; incidental finding of asymptomatic CSVD at brain magnetic resonance imaging (MRI). According to Fazekas scale, subjects were classified by presence of white matter hyperintensities in periventricular region (pvWMHs), deep white matter region (dWMHs), or both (d+pvWMHs). We compared the concentration of hemoglobin species and tissue oxygen saturation (StO_2) among these groups. The study included 20 subjects, median age 67.5 (IQR 61–78) years old (6 without WMHs, 5 with pvWMHs, 9 with d+pvWMHs). Subjects with d+pvWMHs had significantly lower StO_2 compared to subjects without WMHs (p = 0.022) or with pvWMHs (p = 0.004). StO_2 < 56.7% indicated the presence of d+pvWMHs with 91% sensitivity and 67% specificity [AUC 91% (CI 95% 78–100%)]. In this preliminary study, cerebral TD-NIRS detected significantly lower StO_2 in subjects with radiological signs of asymptomatic CSVD. Further studies are needed to evaluate if StO_2 might represent a marker of asymptomatic CSVD.

Keywords: microcirculation dysfunction in cerebral small vessel disease; asymptomatic cerebral small vessel disease; NIRS in cerebrovascular diseases; oxygen saturation in cerebral small vessel disease; novel applications of time-domain near-infrared spectroscopy; TD-NIRS; time-resolved near-infrared spectroscopy; neuroimaging of leukoarayiosis; Fazekas scale and white matter hyperintensites; NIRS in healthy subjects

Citation: Giacalone, G.; Zanoletti, M.; Re, R.; Contini, D.; Spinelli, L.; Torricelli, A.; Roveri, L. Time-Domain Near-Infrared Spectroscopy in Subjects with Asymptomatic Cerebral Small Vessel Disease. *Appl. Sci.* **2021**, *11*, 2407. https://doi.org/10.3390/app11052407

Academic Editor: Herbert Schneckenburger

Received: 11 January 2021
Accepted: 5 March 2021
Published: 9 March 2021

1. Introduction

Cerebral small vessel disease (CSVD) is a structural and functional disorder of brain microcirculation leading to progressive tissue damage visible at brain autopsy and with computed tomography/magnetic resonance imaging (CT/MRI) scan [1]. CSVD accounts for 25% of ischemic strokes, is frequently found in most hemorrhagic strokes and contributes up to 50% of dementias worldwide, representing an extremely important health issue [1].

In CSVD, the vascular walls of arterioles, capillaries and venules undergoe morphological changes, such as arteriolosclerosis, lipohyalinosis, fibrinoid necrosis, and venous collagenosis, that disturb blood flow patterns in microcirculation and local oxygen delivery [1–3]. In addition, blood-brain barrier dysfunction can cause the leakage of fluids,

proteins and other plasma constituents into the perivascular tissues, which might increase interstitial fluid, stiffen arteriole and venule walls [1]. The effects of these phenomena impair cerebrovascular reactivity, vascular pulsatility, hemodynamic blood flow redistribution, leading to inefficient oxygen and nutrient transport, and to neurovascular dysfunction. Cerebral infarction may finally result from arteriolar occlusion and hemodynamic insufficiency phenomena.

Asymptomatic CSVD, defined as neuroimaging evidence of CSVD prior to the development of any overt clinical symptoms, is common in adult healthy subjects regardless of associated vascular risk factors [4]. Usually, the clinical manifestation of the disease becomes evident with accumulation of brain lesions. Imaging markers of CSVD, including lacunes, white matter hyperintensities (WMHs), enlarged perivascular spaces (EPVS) and cerebral microbleeds (CMBs) are commonly observed on brain MRI in healthy individuals. The reported prevalence of these lesions in elderly populations varies across different studies, ranging from 8% to 33% for lacunes [5], 3% to 34% for CMBs [6], and 39% to 96% for WMHs [7]. Fazekas scale, which classifies WMHs in periventricular and deep white regions, is one of the most used scoring systems to classify CSVD [8]. The typical lesions of CSVD are indeed located in the white matter of centrum semiovale, in periventricular regions and in deep structures, even though the functional alteration of microcirculation affects both cortical and white matter arterioles, capillaries and venules.

The detection of meaningful biomarkers of asymptomatic CSVD is one among the unmet needs of CSVD. Advanced optical devices, such as time-domain near infrared spectroscopy (TD-NIRS), might provide useful information about oxygenation of cerebral microcirculation in the superficial layers in a non-invasive way, with limited costs and overcoming some limitations of previous NIRS systems, such as continuous-wave NIRS. In particular, advanced optical devices, such as TD-NIRS and frequency-domain NIRS (FD-NIRS), allow to recover the absolute concentrations of hemoglobin species, the value of tissue oxygen saturation (StO_2) and to reduce the contamination from extra-cerebral layers. In TD-NIRS with single source–detector pair, the effect of extra-cerebral layers can be marginal even if fitting with homogeneous model is used [9]. TD-NIRS and FD-NIRS are able to provide reproducible measurements of cerebral hemoglobin species and StO_2 [10,11]. Besides, previous studies have shown that advanced optical devices can detect hemodynamic changes in ischemic stroke, among which different concentrations of hemoglobin species and tissue oxygen saturation values in patients with acute ischemic stroke compared to controls and in ischemic areas respect to non-ischemic regions [10–18].

In this study we hypothesize that probing the oxygenation of microcirculation of the superficial layers might provide indirect information about the presence of CSVD. We aimed to explore if TD-NIRS might correlate with asymptomatic CSVD documented by brain MRI by comparing the concentration of hemoglobin species and StO_2 between subjects with and without radiological signs of CSVD.

2. Materials and Methods

The study received approval by the Institutional Ethical Committee and by the Ministry of Health and was conducted in compliance with the Declaration of Helsinki and written informed consent was obtained from each subject. We retrospectively selected healthy subjects from a previous TD-NIRS study [10] meeting the following criteria: (a) age $\geq$ 55 years old; (b) no clinical history of brain disease; (c) normal neurological examination; (d) absence of stenosis > 50% of extra- or intra-cranial arteries; (e) available brain magnetic resonance imaging (MRI).

The burden of CSVD was assessed according to Fazekas score on brain MRI sequences including axial diffusion-weighted imaging (DWI), T2-weighted, fluid-attenuated inversion recovery (FLAIR), gradient echo, and T1-weighted sequences [8]. The scale divides the white matter hyperintensities in periventricular (Fazekas-pv) and deep white matter (Fazekas-d) accounting for size and confluence of lesions. Periventricular lesions (pvWMHs) scores are: 0 = absent; 1 = “caps” or pencil-thin lining; 2 = smooth “halo”; 3 =

irregular periventricular signal extending into the deep white matter. Deep white matter lesions (dWMHs) scores are: 0 = absent; 1 = punctate foci; 2 = beginning confluence; 3 = large confluent area. Subjects were classified according to Fazekas-pvWMHs and Fazekas-dWMHs score in 4 groups (Fazekas groups): "noWMHs" group included subjects with pvWMHs and dWMHs score 0; "pvWMHs" included subjects with pvWMHs score ≥ 1 and dWMHs score 0; "dWMHs" included subjects with dWMHs score ≥ 1 and pvWMHs score 0; "d+pvWMHs" included subjects with pvWMHs and dWMHs score ≥ 1.

TD-NIRS measurements were performed in resting conditions, with the subject lying with an angle-of-bed inclination of 30°. TD-NIRS measurements were obtained by placing a pair of illuminating and collecting optical fibers in selected standard positions of frontal, central and parietal brain regions of each hemisphere using an EEG cap (g.EEGcap, g.tec medical engineering GmbH, Schiedlberg, Austria) according to the 10-10 international positioning system (F3-F5, C3-C1, P3-P5 for the left hemisphere and F4-F6, C4-C2, P4-P6 for the right hemisphere). These positions were chosen in the previous TD-NIRS study [10] for two main reasons: (a) to gather standardized information about equidistant areas in the territory supplied by middle cerebral artery [19]; (b) to probe both primary and secondary cortices according to probabilistic anatomical correlation of 10-10 international system to the brain cortex [20]. The recording session consisted of three sets of measurements for each position of interest. We obtained concomitant non-invasive arterial blood pressure, heart rate, SpO_2 and peripheral blood Hb concentrations for each subject.

TD-NIRS data were acquired by means of a device designed and developed at Department of Physics of Politecnico di Milano [10]. The light sources are three pulsed diode lasers working at 690 nm, 785 nm and 830 nm, respectively (mod. LDH series, PicoQuant GmbH, Berlin, Germany) and at 80 MHz repetition rate. Laser pulses are injected into the tissue by multimode graded index optical fibers (100/140 µm core/cladding diameter) paying attention in maintaining the power density below the maximum permissible exposure of 2 mW/mm^2 thanks to a spacer placed at the tip of the probe. Photons are collected from the tissue in reflectance mode by means of a custom-made three furcate fiber bundle made of graded index plastic fibers (1 mm core diameter, 0.29 NA; mod. OM-GIGA POF, Luceat Srl, Brescia, Italy) and then detected by three hybrid photomultipliers (mod. HPM-100-50, Becker-Hickl, GmbH, Berlin, Germany), each dedicated to a specific wavelength by using band pass filters centered at 690 nm, 785 nm and 830 nm (mod. Hard Coated OD4, 10 nm Bandpass Filters, Edmund Optics GmbH, Mainz, Germany). Finally, three Time Correlated Single Photon Counting (TCSPC) boards acquire the distributions of photon time of flight that is the TD-NIRS signal or curves. The Instrument Response Function (IRF), obtained by facing the injection fiber with the collection fiber, features a Full Width at Half Maximum (FWHM) < 200 ps.

TD-NIRS data at each wavelength were fitted with the solution of the diffusion equation for semi-infinite homogenous media after convolution with the IRF. In particular, a spectral constraint during the inversion procedure was employed, by exploiting the empirical spectral dependence for the reduced scattering obtained by Mie theory, and the Beer's law to express the absorption coefficient as a linear superposition of the specific absorption of HbR, HbO and water. Further details in data analysis and quality controls (e.g., on number of detected photons, time drift of laser pulses, robustness of fitting procedure) are described in a previous study [10]. At each recording session, the values of HbR, HbO, HbT and StO_2 of every single position were averaged across three sets of measurements. Since no differences in hemodynamic parameters have been detected between hemispheres in healthy subjects in a previous study [10], we calculated a grand average of concentration of HbR, HbO, HbT and StO_2 across the six measured positions for final analyses. The measurement set-up is also described in Figure 1.

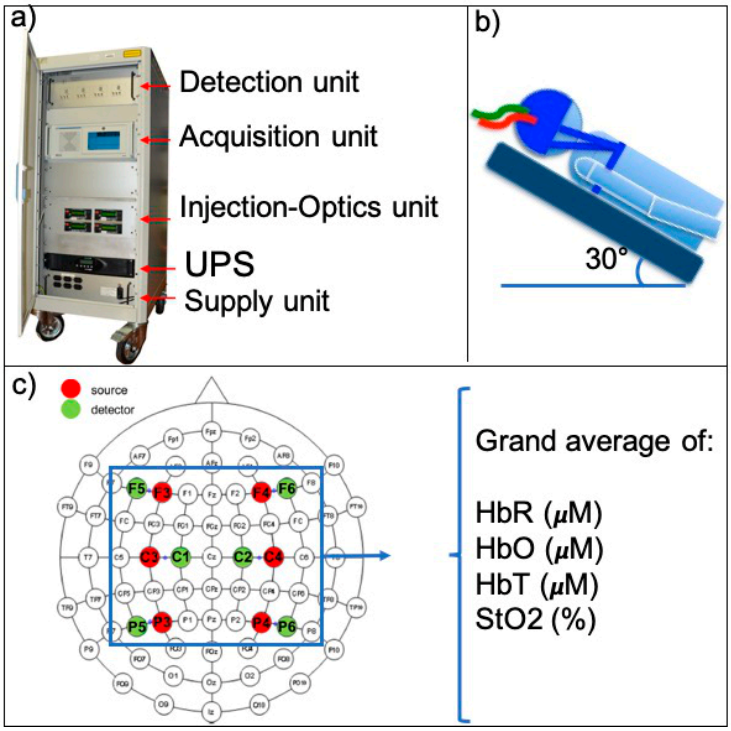

Figure 1. Time-Domain Near-Infrared spectroscopy (TD-NIRS) measurement set-up. (**a**) TD-NIRS device; (**b**) head-of-bed inclination; (**c**) probed positions on the scalp and grand average of recovered concentrations of HbR, HbO, HbT and of StO_2 value.

Clinical and demographic variables were compared among groups using χ^2 (or Fisher exact test when necessary) for categorical variables, independent sample Kruskal-Wallis test for continuous variables. Comparisons for hemoglobin species (HbR, HbO, HbT) and StO_2 among groups were performed using independent sample Kruskal-Wallis test with pairwise comparisons. Multiple linear regression analysis was performed using results with $p < 0.1$ as independent variables in univariate analysis. Data analysis was performed with SPSS Statistics for Macintosh, version 20.0 (Armonk: IBM Corp., Armonk, NY, USA).

3. Results

The study cohort comprised 20 subjects [median age 67.5 (IQR 61–78) years old] of which 6 subjects had noWMHs, 5 subjects had pvWMHs, and 9 subjects had d+pvWMHs. There were no subjects belonging to dWMHs group since all subjects with dWMHs also had pvWMHs.

Demographic features, vascular risk factors, clinical and laboratory parameters including arterial blood pressure, heart rate, SpO_2, mean peripheral blood hemoglobin concentration of the three groups are reported in Table 1.

There was a significant difference of StO_2 values among groups ($p = 0.007$) (Table 2). In pairwise comparisons, subjects with noWMHs had StO_2 values comparable to subjects with pvWMHs ($p = 0.53$) while subjects with d+pvWMHs had significantly lower StO_2 compared to noWMHs ($p = 0.022$) and to pvWMHs ($p = 0.004$).

We performed an explorative multiple linear regression analysis with increasing extension of WMHs (Fazekas groups) as dependent variable (0 = no WMHs, 1 = pvWMHs, 2 = d+pvWMHs). According to univariate analysis, age, arterial hypertension, smoking, SpO_2 and StO_2 were entered as independent variables (all independent variables entered into the equation at the same time as "enter" method). We calculated the power of the linear multiple regression analysis (fixed model, R^2 increase) according to the following characteristics: sample size = 20, alpha = 0.05, number of predictors = 5, alpha\beta ratio = 1. The estimated power according to large, medium and low effect sizes f^2 (respectively,

$f^2 = 0.35$, $f^2 = 0.15$, $f^2 = 0.02$) were respectively 86%, 73%, 54%. Variance inflation factors below 1.5 excluded the presence of collinearity. Independence of residuals was confirmed by Durbin-Watson statistic. Homoscedasticity was evaluated by visual inspection of a plot of standardized residuals versus standardized predicted values. The normality of the distribution of residuals was assessed by visual inspection of a normal P-P plot. The regression model significantly predicted Fazekas groups F (5, 19) = 8.8, $p = 0.001$ and had a $R^2 = 76\%$. According to the linear regression model, StO_2, age and arterial hypertension were significantly associated with increasing extension of WMHs (Table 3).

Table 1. Comparison of demographic and clinical characteristics according to Fazekas groups.

	noWMHs $n = 6$	pvWMHs $n = 5$	d+pvWMHs $n = 9$	p
Age (years) *	59 (56–61)	68 (67–78)	70 (70–77)	0.015
Gender (M/F)	83/17%	80/20%	44/56%	0.22
Arterial hypertension	17%	20%	67%	0.09
Diabetes mellitus	0%	40%	33%	0.23
Smoking	33%	0%	0%	0.07
Hypercholesterolemia	17%	20%	11%	0.9
Atrial fibrillation	0%	0%	22%	0.26
Migraine	0%	20%	11%	0.54
MAP (mmHg) *	95 (88–97)	90 (87–90)	90 (87–103)	0.63
Heart rate (beats/min) *	64 (60–70)	65(60–73)	71 (65–82)	0.60
SpO_2 (%) *	99 (98–99)	97 (96–97)	98 (98–99)	0.06
Hb (g/dl) *	13.9 (1.4)	13.9 (0.5)	13.2 (1.2)	0.56

* Median (IQR); MAP: mean arterial blood pressure; SpO_2: peripheral pulse oximetry; Hb: blood hemoglobin concentration.

Table 2. Comparison of concentrations of hemoglobin species and StO_2 values in Fazekas groups.

	noWMHs $n = 6$	pvWMHs $n = 5$	d+pvWMHs $n = 9$	p
HbR (μM)	23.7 (22.1–25.3)	19.0 (18.6–19.1)	23.0 (17.9–25.8)	0.32
HbO (μM)	34.1 (31.9–35.6)	29.8 (26.5–35.2)	26.9 (25.7–29.3)	0.26
HbT (μM)	57.5 (54.8–61.0)	48.8 (45.2–54.3)	51.1 (44.2–55.1)	0.28
StO_2 (%)	58.8 (57.5–59.5)	61.1 (58.6–61.6)	54.8 (53.2–57.3)	0.007

The values are reported as median (IQR). p: p-value of statistical significance of differences among groups according to independent sample Kruskal-Wallis test.

Table 3. Binomial linear regression (dependent variable: Fazekas groups).

Independent Variables	t	Beta	p
StO_2	−2.5	−0.96 (−0.18–−0.015)	0.023
Age	3.7	0.06 (0.025–0.093)	0.002
Arterial hypertension	2.3	0.55 (0.040–1.01)	0.037
Smoking	−1.5	−0.63 (−1.5–0.26)	0.152
SpO_2	2.0	0.21 (−0.01–0.43)	0.066
Constant	−1.6	−18.1 (−42.9–6.7)	

In an explorative ROC analysis, grouping together noWMHs and pvWMHs subjects, a cut-off of cerebral $StO_2 < 56.7\%$ indicated the presence of d+pvWMHs with 91% sensitivity and 67% specificity [AUC 91% (CI 95% 78–100%)] (Figure 2).

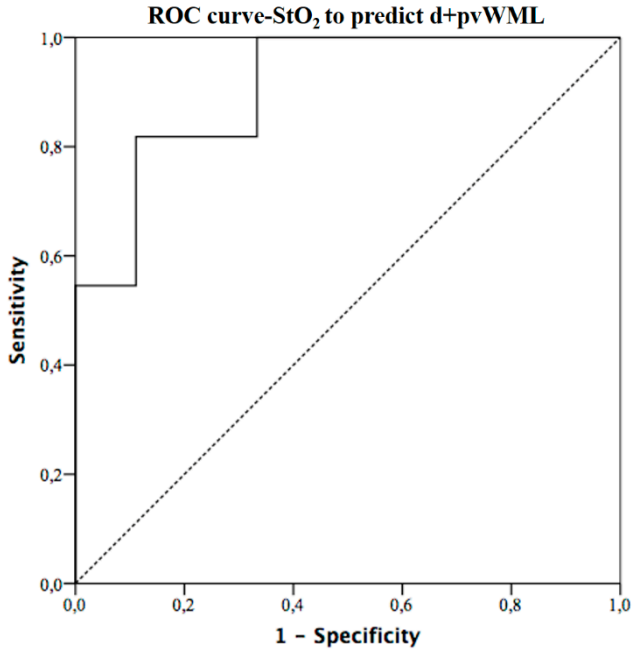

Figure 2. ROC curve sensitivity and specificity of StO_2 in predicting d+pvWMHs.

4. Discussion

The present study is the first attempt to assess oxygenation of microcirculation of cerebral outer layers by means of TD-NIRS in subjects with asymptomatic CSVD. Considering that CSVD is a structural and functional disorder of brain microcirculation, techniques that investigate the microcirculation might provide complementary information about early changes in asymptomatic CSVD. Some of the limitations of previous NIRS techniques have been overcome by TD-NIRS and FD-NIRS, which can better discriminate the extracerebral contribution to the signal and provide absolute and reproducible concentration of hemoglobin species and StO_2. TD-NIRS investigates the oxygenation of microcirculation of cerebral outer layers that is functionally and anatomically connected to the microcirculation of subcortical and deep white matter on the arterial and venous side. Indeed, subcortical and deep white matter regions receive arterial blood through medullary arteries coming from leptomeningeal spaces [21] and the venous drainage of subcortical white matter is directed to cortical pial veins [22]. While the radiological signs of CSVD are mainly located in deep and periventricular regions, it might be conceivable that the microcirculatory impairment or consequences are global. Therefore, the study of oxygenation of cerebral outer layers with TD-NIRS might indirectly reflect the presence of radiological signs of CSVD. According to our explorative data, cerebral oximetry with TD-NIRS was able to detect significantly lower cerebral StO_2 in a cohort of subjects with incidental radiological signs of asymptomatic CSVD located in periventricular and deep white matter regions compared to individuals without white matter hyperintensities. We also observed that StO_2 did not differ between subjects without WMHs and with WMHs only in periventricular regions. This could be due to the more limited extension of CSVD or to an intrinsic limitation of TD-NIRS to detect signals from the deeper arterial and venous blood systems supply of periventricular regions.

Previous NIRS studies have shown that StO_2 is a highly reproducible parameter with a fairly restricted coefficient of variation among subjects [10,11]. Previous TD-NIRS data suggested that HbR, HbO, HbT and, to a lesser extent, StO_2 values reduce with increasing age [10]. In our cohort, as expected, subjects with noWMHs were younger than individuals with pvWMHs and d+pvWMHs. However, in multiple linear regression analysis including age as independent variable, StO_2 remained statistically significantly associated with increasing extension of WMHs.

In this exploratory study, we assessed subjects with only minor signs of CSVD without functional impact. Although incidental radiological signs of CSVD have a high prevalence in healthy subjects, it remains to determine what proportion of asymptomatic CSVD will progress into cognitive impairment, dementia or stroke. Some population studies have shown progression of WMHs and of cognitive decline not only in subjects with confluent alterations, but also in individuals with punctate lesions [23,24]. Longitudinal studies might contribute to identify subjects at high probability of becoming symptomatic to whom possibly offer future treatment strategies at an early asymptomatic phase of the disease. Our preliminary data suggest that minor, asymptomatic radiological CSVD might be associated with low StO_2 values, that might represent a sign of dysfunction of cerebral microcirculation.

We acknowledge that this study has a number of limitations among which the very small sample size, the gender unbalance between d+pvWMHs and the other groups and the retrospective nature of the study, which can reduce the general validity of findings. Therefore, these preliminary results need to be confirmed in a larger cohort of subjects along with longitudinal test of cognitive functions and brain MRI imaging. The absence of a concomitant measurement of cerebral blood flow in microcirculation represents a limit to a better understanding. The concomitant use in future studies of diffuse correlation spectroscopy might be a valuable strategy to get further insight in the underlying patho-physiological phenomena. We also acknowledge that probing the superficial layers of cerebral tissue in resting conditions might give only indirect and incomplete information about the global status of cerebral microcirculation. The exploratory nature of this study does not allow further speculation on the possible causes of our finding. Therefore, the results may serve merely to generate hypothesis. Finally, we are aware that the use of a homogenous model for TD-NIRS data analysis instead of a two-layer algorithm is a possible limitation of our study. In a previous multi-laboratory study [25], a substantial agreement was found, both in simulations and in vivo measurements, between TD-NIRS absorption coefficients retrieved from the homogenous model and the estimate of the absorption coefficient in the lower layer derived by exploiting a two-layer model.

In summary, this pilot study detected significantly low StO_2 values in subjects with asymptomatic CSVD. This result suggests that the association of low StO_2 with CSVD should be further investigated.

Supplementary Materials: The following are available online at https://www.mdpi.com/2076-3417/11/5/2407/s1.

Author Contributions: Conceptualization, G.G. and L.R.; Data curation, G.G., M.Z., R.R., D.C., L.S., A.T. and L.R.; Formal analysis, G.G., M.Z., R.R., D.C., L.S., A.T. and L.R.; Investigation, G.G. and L.R.; Methodology, G.G. and L.R.; Resources, G.G., M.Z., R.R., D.C., L.S., A.T. and L.R.; Software, M.Z., R.R., D.C., L.S. and A.T.; Writing—original draft, G.G. and L.R.; Writing—review & editing, M.Z., R.R., D.C., L.S. and A.T. All authors have read and agreed to the published version of the manuscript.

Funding: This research received no external funding.

Institutional Review Board Statement: The study was conducted according to the guidelines of the Declaration of Helsinki, and approved by the Local Ethics Committee of San Raffaele Hospital with code TD-NIRS 1.0 on 7th September 2015.

Informed Consent Statement: Informed consent was obtained from all subjects involved in the study.

Data Availability Statement: The dataset is available in Supplementary Data.

Conflicts of Interest: The authors declare no conflict of interest.

References

1. Wardlaw, J.M.; Smith, C.; Dichgans, M. Small vessel disease: Mechanisms and clinical implications. *Lancet Neurol.* **2019**, *18*, 684–696. [CrossRef]
2. Pantoni, L. Cerebral small vessel disease: From pathogenesis and clinical characteristics to therapeutic challenges. *Lancet Neurol.* **2010**, *9*, 689–701. [CrossRef]

3. Østergaard, L.; Engedal, T.S.; Moreton, F.; Hansen, M.B.; Wardlaw, J.M.; Dalkara, T.; Markus, H.S.; Muir, K.W. Cerebral small vessel disease: Capillary pathways to stroke and cognitive decline. *J. Cereb. Blood Flow. Metab.* **2016**, *36*, 302–325. [CrossRef] [PubMed]
4. Das, A.D.; Regenhardt, R.W.; Vernooij, M.W.; Blacker, D.; Charidimou, A.; Viswanathan, A. Asymptomatic Cerebral Small Vessel Disease: Insights from Population-Based Studies. *J. Stroke* **2019**, *21*, 121–138. [CrossRef]
5. Vermeer, S.E.; Longstreth, W.T.; Koudstaal, P.J. Silent brain infarcts: A systematic review. *Lancet Neurol.* **2007**, *6*, 611–619. [CrossRef]
6. Greenberg, S.M.; Vernooij, M.W.; Cordonnier, C.; Viswanathan, A.; Al-Shahi Salman, R.; Warach, S.; Launer, L.J.; Van Buchem, M.A.; Breteler, M.M. Microbleed Study Group Cerebral microbleeds: A guide to detection and interpretation. *Lancet Neurol.* **2009**, *8*, 165–174. [CrossRef]
7. Prins, N.D.; Scheltens, P. White matter hyperintensities, cognitive impairment and dementia: An update. *Nat. Rev. Neurol.* **2015**, *11*, 157–165. [CrossRef]
8. Fazekas, F.; Chawluk, J.B.; Alavi, A.; Hurtig, H.I.; Zimmerma, R.A. MR signal abnormalities at 1.5 T in Alzheimer's dementia and normal aging. *Am. J. Neuroradiol.* **1987**, *8*, 421–426. [CrossRef] [PubMed]
9. Giusto, A.; D'Andrea, C.; Spinelli, L.; Contini, D.; Torricelli, A.; Martelli, F.; Zaccanti, G.; Cubeddu, R. Monitoring absorption changes in a layered diffusive medium by white-light time-resolved reflectance spectroscopy. *IEEE Trans. Instrum. Meas.* **2010**, *59*, 1925–1932. [CrossRef]
10. Giacalone, G.; Zanoletti, M.; Contini, D.; Re, R.; Spinelli, L.; Roveri, L.; Torricelli, A. Cerebral time domain-NIRS: Reproducibility analysis, optical properties, hemoglobin species and tissue oxygen saturation in a cohort of adult subjects. *Biomed. Opt. Express* **2017**, *8*, 4987. [CrossRef]
11. Hallacoglu, B.; Sassaroli, A.; Wysocki, M.; Guerrero-Berroa, E.; Schnaider Beeri, M.; Haroutunian, V.; Shaul, M.; Rosenberg, I.H.; Troen, A.M.; Fantini, S. Absolute measurement of cerebral optical coefficients, hemoglobin concentration and oxygen saturation in old and young adults with near-infrared spectroscopy. *J. Biomed. Opt.* **2012**, *17*, 081406. [CrossRef] [PubMed]
12. Flint, A.C.; Bhandari, S.G.; Cullen, S.P.; Reddy, A.V.; Hsu, D.P.; Rao, V.A.; Patel, M.; Pombra, J.; Edwards, N.J.; Chan, S.L. Detection of anterior circulation large artery occlusion in ischemic stroke using noninvasive cerebral oximetry. *Stroke* **2018**, *49*, 458–460. [CrossRef] [PubMed]
13. Ritzenthaler, T.; Cho, T.H.; Mechtouff, M.; Ong, E.; Turjman, F.; Robinson, F.; Berthezène, Y.; Nighoghossian, N. Cerebral near-infrared spectroscopy a potential approach for thrombectomy monitoring. *Stroke* **2017**, *48*, 3390–3392. [CrossRef]
14. Delgado-Mederos, R.; Gregori-Pla, C.; Zirak, P.; Blanco, I.; Dinia, L.; Marín, R.; Durduran, T.; Martí-Fàbregas, J. Transcranial diffuse optical assessment of the microvascular reperfusion after thrombolysis for acute ischemic stroke. *Biomed. Opt. Express* **2018**, *9*, 1262–1271. [CrossRef]
15. Durduran, T.; Zhou, C.; Edlow, B.L.; Yu, G.; Choe, R.; Kim, M.N.; Cucchiara, B.L.; Putt, M.E.; Shah, Q.; Kasner, S.E.; et al. Transcranial optical monitoring of cerebrovascular hemodynamics in acute stroke patients. *Opt. Express* **2009**, *17*, 3884–3902. [CrossRef]
16. Gregori-Pla, C.; Blanco, I.; Camps-Renom, P.; Zirak, P.; Serra, I.; Cotta, G.; Maruccia, F.; Prats-Sánchez, L.; Martínez-Domeño, A.; Busch, D.R.; et al. Early microvascular cerebral blood flow response to head-of-bed elevation is related to outcome in acute ischemic stroke. *J. Neurol.* **2019**, *266*, 990–997. [CrossRef] [PubMed]
17. Gregori-Pla, C.; Delgado-Mederos, R.; Cotta, G.; Giacalone, G.; Maruccia, F.; Avtzi, S.; Prats-Sánchez, L.; Martínez-Domeño, A.; Camps-Renom, P.; Martí-Fàbregas, J.; et al. Microvascular cerebral blood flow fluctuations due to periodic apneas in acute ischemic stroke. *Neurophotonics* **2019**, *6*, 025004. [CrossRef] [PubMed]
18. Giacalone, G.; Zanoletti, M.; Re, R.; Germinario, B.; Contini, D.; Spinelli, L.; Torricelli, A.; Roveri, L. Time-domain near-infrared spectroscopy in acute ischemic stroke patients. *Neurophotonics* **2019**, *6*, 015003. [CrossRef]
19. Tatu, L.; Moulin, T.; Bogousslavsky, J.; Duvernoy, H. Arterial territories of the human brain: Cerebral hemispheres. *Neurology* **1998**, *50*, 1699–1708. [CrossRef]
20. Koessler, L.; Maillard, L.; Benhadid, A.; Vignal, J.P.; Felblinger, J.; Vespignani, H.; Braun, M. Automated cortical projection of EEG sensors: Anatomical correlation via the international 10-10 system. *Neuroimage* **2009**, *46*, 64–72. [CrossRef]
21. Nonaka, H.; Akima, M.; Hatori, T.; Nagayama, T.; Zhang, Z.; Ihara, F. Microvasculature of the human cerebral white matter: Arteries of the deep white matter. *Neuropathology* **2003**, *23*, 111–118. [CrossRef] [PubMed]
22. Tong, L.S.; Guo, Z.N.; Ou, Y.B.; Yu, Y.N.; Zhang, X.C.; Tang, J.; Zhang, J.H.; Lou, M. Cerebral venous collaterals: A new fort for fighting ischemic stroke? *Prog. Neurobiol.* **2018**, *163–164*, 172–193. [CrossRef] [PubMed]
23. Schmidt, R.; Berghold, A.; Jokinen, H.; Gouw, A.A.; van der Flier, W.M.; Barkhof, F.; Scheltens, P.; Petrovic, P.; Madureira, S.; Verdelho, A.; et al. White matter lesion progression in LADIS: Frequency, clinical effects, and sample size calculations. *Stroke* **2012**, *43*, 2643–2647. [CrossRef]
24. Van Dijk, E.J.; Prins, N.D.; Vrooman, H.A.; Hofman, A.; Koudstaal, P.J.; Breteler, M.M.B. Progression of cerebral small vessel disease in relation to risk factors and cognitive consequences: Rotterdam scan study. *Stroke* **2008**, *39*, 2712–2719. [CrossRef]
25. Farina, A.; Torricelli, A.; Bargigia, I.; Spinelli, L.; Cubeddu, R.; Foschum, F.; Jäger, M.; Simon, E.; Fugger, O.; Kienle, A.; et al. In vivo Multilaboratory investigation of the optical properties of the human head. *Biomed. Opt. Express* **2015**, *6*, 2609–2623. [CrossRef] [PubMed]